EUROPEAN ORGANIZATION FOR NUCLEAR RESEARCH

CERN-PPE/93-74
29.04.1993

ANTIPROTON-PROTON ANNIHILATION AT REST INTO $\omega\pi^0\pi^0$

C. Amsler[13], D. Armstrong[1], I. Augustin[7], C.A. Baker[4], B.M. Barnett[10], C.J. Batty[4], K. Beuchert[2], P. Birien[1], J. Bistirlich[1], P. Blüm[7], R. Bossingham[1], H. Bossy[1], K. Braune[11], J. Brose[10], D.V. Bugg[8], M. Burchell[5,a], T. Case[1], S.U. Chung[10,b], A. Cooper[8], K.M. Crowe[1], H.P. Dietz[11], S. v. Dombrowski[13,c], M. Doser[5], W. Dünnweber[11], D. Engelhardt[7], M. Englert[11], M.A. Faessler[11], C. Felix[11], G. Folger[11], R. Hackmann[10], R.P. Haddock[9], F.H. Heinsius[6], N.P. Hessey[5], P. Hidas[3], P. Illinger[11], D. Jamnik[11,d], Z. Jávorfi[3], H. Kalinowsky[10], B. Kämmle[6], T. Kiel[6], J. Kisiel[11,e], E. Klempt[10], M. Kobel[5], H. Koch[2], C. Kolo[11], K. Königsmann[11], M. Kunze[2], R. Landua[5], J. Lüdemann[2], H. Matthaey[2], M. Merkel[10], J.P. Merlo[10], C.A. Meyer[13], L. Montanet[5], A. Noble[13], F. Ould-Saada[13], K. Peters[2], G. Pinter[3], S. Ravndal[2], J. Salk[2], A.H. Sanjari[8,f], E. Schäfer[10], B. Schmid[13,g], P. Schmidt[6], S. Spanier[10], C. Straßburger[10], U. Strohbusch[6], M. Suffert[12], D. Urner[13], C. Völcker[11], F. Walter[10], D. Walther[2], U. Wiedner[6], N. Winter[7], J. Zoll[5], Č. Zupančič[11].

Crystal Barrel Collaboration

1) *University of California, LBL, Berkeley, CA 94720, USA*
2) *Universität Bochum, D-4630 Bochum, Germany*
3) *Academy of Science, H-1525 Budapest, Hungary*
4) *Rutherford Appleton Laboratory, Chilton, Didcot OX11 0QX, UK*
5) *CERN, CH-1211 Genève, Switzerland*
6) *Universität Hamburg, D-2000 Hamburg, Germany*
7) *Universität Karlsruhe, D-7500 Karlsruhe, Germany*
8) *Queen Mary and Westfield College, London E1 4NS, UK*
9) *University of California, Los Angeles, CA 90024, USA*
10) *Universität Mainz, D-6500 Mainz, Germany*
11) *Universität München, D-8000 München, Germany*
12) *Centre de Recherches Nucléaires, F-67037 Strasbourg, France*
13) *Universität Zürich, CH-8001 Zürich, Switzerland*

Submitted to Physics Letters B

---

a) Now at University of Kent, Canterbury, UK
b) On leave of absence from BNL, Upton, NY, USA
c) M.Sc. thesis of S.v. Dombrowski
d) On leave of absence from the University of Ljubljana, Ljubljana, Slovenia
e) On leave of absence from the University of Silesia, Katowice, Poland
f) Now at the State University of New York, Stony Brook, NY, USA
g) Now at the University of California, Irvine, CA, USA

Abstract

The annihilation channel $\overline{p}p \rightarrow \omega\pi^0\pi^0$, where ω decays to $\pi^0\gamma$, was studied with antiprotons stopped in liquid hydrogen. This reaction is dominated by the production of $b_1^0(1235)$ with contributions from $f_2(1270)$ and the $\pi\pi$ S-wave. The branching ratio for $\overline{p}p \rightarrow \omega\pi^0\pi^0$ is (2.00 $\pm$ 0.21) % of all annihilations. The branching ratios for $b_1^0(1235)\pi^0$ ($b_1 \rightarrow \omega\pi^0$) and $f_2(1270)\omega$ ($f_2 \rightarrow \pi^0\pi^0$) are (0.92 $\pm$ 0.11) % and (0.57 $\pm$ 0.07) % of all annihilations, respectively. Upper limits for the production of vector mesons decaying to $\omega\pi$ are given and the $\pi\pi$ mass distribution around 1 GeV is discussed.

The reaction $\overline{p}p \to \omega\pi^0\pi^0$ has not been studied previously due to the lack of experiments having efficient detection for final states with several photons. This process is of interest to search for vector mesons decaying to $\omega\pi^0$ and for scalar mesons decaying to $\pi^0\pi^0$. Under the assumption that S-state annihilation dominates in liquid hydrogen [1], only the $^3S_1$ initial $\overline{p}p$ atomic state contributes to $\omega\pi^0\pi^0$. Furthermore, the $\pi^0\pi^0$ amplitudes are purely isoscalar. In contrast, the reaction $\overline{p}p \to \omega\pi^+\pi^-$ is rather complex due to contributions from both $^1S_0$ and $^3S_1$ initial states and the strong isovector $\pi\pi$ P-wave (ρ meson). The final state $\omega\pi^+\pi^-$ (where ω decays to $\pi^+\pi^-\pi^0$) has been investigated in bubble chambers [2, 3] and by the ASTERIX collaboration in gaseous hydrogen where P-state annihilation contributes strongly [4]. The analysis of $\omega\pi^+\pi^-$ required, apart from $b_1(1235)$, a radial excitation of the ρ meson around 1250 MeV decaying to $\omega\pi$ [3]. Another radial excitation, $\rho(1450)$, has also been reported in e^+e^- annihilation into $\omega\pi$ [5].

Potential models of the $\overline{N}N$ interaction predict a band of 0^{++}, 1^{--}, and 2^{++} deeply bound isoscalar $\overline{N}N$ states [6]. The $f_2(1520)$, observed in the annihilation channel $\overline{p}p \to f_2\pi^0$ [7, 8, 9], has been interpreted as the 2^{++} member of this band [10]. With $f_2(1520)$ setting the mass scale, one would then expect the 0^{++} partner to lie around 1100 MeV [10]. An analysis of the $\omega\pi^+\pi^-$ final states with 2400 events indeed required a scalar structure around 1115 MeV in the $\pi\pi$ S-wave, although the fit was rather insensitive to the precise mass value [2]. An isoscalar 0^{++} state with a width of 80 MeV has been reported at 1080 MeV in the $\pi^+\pi^-$ mass spectrum of the reaction $\overline{p}p \to \rho^0\pi^+\pi^-$ [11]. An isoscalar with a width of 117 MeV has also been reported at 1107 MeV in the reaction $\overline{p}n \to \rho^-\pi^+\pi^-$ but spin and parities (0^{++} or 2^{++}) were not determined [12].

In order to clarify the situation, we have studied with 16'852 events the reaction $\overline{p}p \to \omega\pi^0\pi^0$ at rest, where ω decays to $\pi^0\gamma$. The experiment was performed with the Crystal Barrel detector on beam line C2 at the Low Energy Antiproton Ring (LEAR) at CERN. Antiprotons with a momentum of 200 MeV/c are stopped in a 4 cm long liquid hydrogen target. A matrix of four silicon counters in front of the target defines and monitors the incident $\bar{p}$ beam (typically 10^4 $\bar{p}$/s). The target is surrounded by two cylindrical proportional wire chambers, a jet drift chamber to detect charged particles and a barrel-shaped calorimeter consisting of 1380 CsI(Tl) crystals, 16 radiation lengths deep, with photodiode readout. The CsI calorimeter covers the polar angles between 12° and 168° with full coverage in azimuth. The useful acceptance for shower detection is $0.95\times4\pi$ sr. The energy calibration is provided by $\pi^0 \to 2\gamma$ decays. The energy resolution is $\sigma/E \sim 2.5$ % for 1 GeV photons and the angular resolution is typically σ = 20 mr in both polar and azimuthal angles. The assembly is located in a solenoidal magnet providing a homogeneous field of 1.5 T parallel to the incident $\bar{p}$ beam. A more detailed description of the apparatus can be found in Ref. [13].

The data presented here are based on 2.21×10^6 annihilations into neutral events which were collected by vetoing events with charged particles, using the inner layers of the jet drift chamber. Events with residual tracks are removed in the offline analysis, leaving 2.05 $\times10^6$ truly neutral events. Events with exactly seven electromagnetic showers with energy deposits exceeding 20 MeV are then selected, and those with a shower induced in the last crystal rows around the beam entrance and exit pipes are removed to suppress energy leakage. These cuts leave 86'839 events. An important background contribution stems from events with six photons (e.g. from $\overline{p}p \to 3\pi^0$), for which one of the showers develops a small neighbouring satellite which is interpreted as an additional shower. These so-called "split-off" events are suppressed by requiring the relative energy deposition of two neighbouring showers, the centroids of which are separated by less than 14°, to be larger than 0.18. This split-off cut reduces the data sample to

57'534 events and removes 99% of the $3\pi^0$ events while rejecting only about 7% of $\omega\pi^0\pi^0$ events. This was established by Monte Carlo simulations based on GEANT3.14 [14] which reproduces electromagnetic split-offs very well.

Next, the total momentum is required to be less than 100 MeV/c and the total energy to lie between 1700 and 1960 MeV. A kinematic fit to the hypothesis $\overline{p}p \rightarrow 3\pi^0\gamma$ is then applied by imposing energy and momentum conservation and three 2γ- invariant masses equal to m_{π^0}. This leaves 27'677 events which satisfy the fit with a confidence level of more than 10%.

Figure 1a shows the energy distribution of the single γ. The low energy peak is due to residual split-offs. For the channel $\overline{p}p \rightarrow \omega\pi^0\pi^0$, one expects the energy of the γ from ω decay to lie in the range 160 to 860 MeV, as observed in fig. 1a. Figure 1b shows the $\pi^0\gamma$ mass distribution after requiring a minimum single γ energy of 160 MeV. A fit between 700 and 900 MeV with a Gaussian superimposed on a second-order polynomial gives for the ω mass:

$$m_\omega = (781.96 \pm 0.13 \pm\ 0.17)\ \text{MeV}. \tag{1}$$

The first error is statistical and the second error reflects the uncertainty in the precise shape of the background. This result is in excellent agreement with the world average (781.95 $\pm$ 0.14 MeV) [15]. The width of the ω signal ($\Gamma = 38.1 \pm 0.3$ MeV) is dominated by the experimental resolution.

Events of the type $\omega\pi^0\pi^0$ are selected by requiring the $\pi^0\gamma$ mass (3 possible combinations) to lie in the mass window between 750 and 815 MeV. About 13% of the events have more than one entry in this mass window. In this case we adopt the combination with the $\pi^0\gamma$ mass closest to m_ω. Simulation shows that this assumption is correct for 95% of the $\omega\pi^0\pi^0$ events. The mass cut leads to 16'852 events consistent with $\omega\pi^0\pi^0$.

The Dalitz plot is shown in fig. 2a and the corresponding mass projections in fig. 2b, c. As will be discussed, the peak in the $\omega\pi$ spectrum is due to $b_1(1235)$ while the $\pi\pi$ spectrum is mainly described by the $\pi\pi$ S-wave. The peak in the $\pi\pi$ mass distribution near 1050 MeV arises from coherent contributions from the $\pi\pi$ S-wave and the tail of $f_2(1270)$.

The background under the ω peak (fig. 1b) arises (i) from genuine $\omega\pi^0\pi^0$ events with more than one $\pi^0\gamma$ combination in the ω mass window or (ii) from 7γ background events, among them wrong $\pi^0 \rightarrow 2\gamma$ combinations, residual split-off events and feedthrough from $4\pi^0$ events with a soft undetected γ. The background (ii) is estimated by counting the fraction of events in side bins left and right from the ω peak with no entry in the ω window. The side bins are chosen as the mass intervals 700 to 732 MeV and 832 to 864 MeV. A small correction is applied to account for the probability for genuine $\omega\pi^0\pi^0$ and background 7γ events to have entries in the side bins and no entry in the ω window. This correction was estimated by Monte Carlo simulation assuming a phase space distribution. The background (ii) contributes 1699 $\pm$ 70 events to the ω mass window. Hence (10.1 $\pm$ 0.4) % of the events in the Dalitz plot are background events. This leaves 15'153$\pm$147 genuine $\omega\pi^0\pi^0$ events, a figure that will be used to extract branching ratios. A background Dalitz plot, generated with events from the ω side bins, appears to be uniformly populated.

The detection and reconstruction probability for the channel $\omega\pi^0\pi^0(\omega \rightarrow \pi^0\gamma)$ is calculated with 10^4 Monte Carlo events generated by GEANT, assuming a phase space distribution. These events are tracked through the detector, reconstructed and submitted to the same cuts as real data. Typical mass resolutions are $\sigma(m^2_{\omega\pi^0}) = 0.031$ GeV^2 and $\sigma(m^2_{\pi^0\pi^0}) = 0.018$ GeV^2. The simulation leads to a detection and reconstruction efficiency $\epsilon = (16.9 \pm 0.4 \pm 0.7)$ %. The first error is statistical while the second error includes systematic uncertainties in the simulation and in the determination of the annihilation vertex. They are described in another publication

dealing with branching ratios for $\overline{p}p$ annihilation into neutral mesons [16]. The reconstruction efficiency will be used below to determine the absolute branching ratio for $\omega\pi^0\pi^0$.

The GEANT sample is however not statistically sufficient to permit a meaningful Dalitz plot analysis. We have therefore generated 10^5 $\omega\pi^0\pi^0$ events with a phase space generator, ignoring detector acceptance and reconstruction efficiency. The ω was allowed to decay with a width consistent with the observed one (Γ = 38.1 MeV). Events with photons softer than 20 MeV or satisfying the split-off criterion were removed, and the $\pi^0\gamma$ mass combination closest to m_ω was adopted as the correct one. This led to 8×10^4 $\omega\pi^0\pi^0$ events. The simulated Dalitz plot population was compared to the corresponding 10^4 GEANT events by using a χ^2 test. Both data sets turned out to be consistent ($\chi^2/\nu = 1.2$ for $\nu = 52$ degrees of freedom, dof) and hence we used the events from the simple phase space generator for the following amplitude analysis.

The experimental Dalitz plot (fig.2a) is analyzed in the helicity formalism [17] in terms of the isobar model in which the $\overline{p}p$ system is assumed to decay to $\omega\pi^0\pi^0$ through two-body intermediate states. The decay chain is assumed to be a succession of two-body decays $A \to BC$ followed by $B \to B_1B_2$ and $C \to C_1C_2$. Suppose an isobar with mass m and spin J decays into two mesons with spins S_1, S_2, total spin S and relative angular momentum L. The amplitude for this decay is given by the matrix [18]

$$A(JLS) = D^J_{\lambda M}(\theta,\phi) < J\lambda|LS0\lambda >< S\lambda|S_1S_2\lambda_1,-\lambda_2 > \times F_L(q) \times BW_L(m) \qquad (2)$$

where the row index $\lambda = \lambda_1 - \lambda_2$ runs over the $(2S_1+1)(2S_2+1)$ helicity states and the column index M over the $2J+1$ magnetic substates; q is the final state momentum and θ and ϕ refer to the decay angles in the isobar rest frame. F_L is the damping factor and BW_L the Breit-Wigner amplitude, both defined below. We shall describe the cascade to $\omega\pi^0\pi^0$ from the initial $\overline{p}p$ state through intermediate isobars by a product of amplitudes A describing successive steps in the cascade.

Owing to parity and C-parity conservation annihilation into $\omega\pi^0\pi^0$ occurs from the $^3S_1(J^{PC} = 1^{--})$ or from the $^1P_1(J^{PC} = 1^{+-})$ $\overline{p}p$ atomic orbitals following $\overline{p}$ capture at rest. As will be shown, a good description of the Dalitz plot population is achieved by assuming S-wave dominance in liquid hydrogen [1] and hence neglecting annihilation from the $^1P_1$ level. The expected contributions are therefore:

1. $\overline{p}p(1^{--}) \to b_1(1235)\pi^0$, $b_1 \to \omega\pi^0$, where b_1 is produced with angular momentum L = 0 or 2 and decays to ω with angular momentum $\ell = 0$ or 2. For $\omega \to \pi^0\gamma$ the relative angular momentum is $\ell' = 1$ (magnetic dipole). Four amplitudes therefore contribute:

$$A_i = A^\omega(111)A^{b_1}(1\ell 1)A^{\overline{p}p}(1L1), \quad i = 1,...,4 \qquad (3)$$

with (L,ℓ) = (0,0), (0,2), (2,0) and (2,2), respectively. Since there are two possible combinations of π^0 and ω to form b_1, A_i must be symmetrized and is in fact the sum of two amplitudes of the form (3).

2. $\overline{p}p(1^{--}) \to \omega(\pi^0\pi^0)_S$ where ω is produced with $L = 0$ or 2 and the $2\pi^0$ system is in a relative S-wave ($\ell = 0$). The two amplitudes are:

$$A_{5,6} = A^\omega(111)A^{\overline{p}p}(1L1). \qquad (4)$$

3. $\overline{p}p(1^{--}) \rightarrow f_2(1270)\omega$, $f_2 \rightarrow \pi^0\pi^0$, where f_2 is produced with $L = 0$ and its decay pions with $\ell = 2$. Although the threshold for this reaction lies above two-nucleon masses, it may nevertheless contribute due to the large width of $f_2(1270)$. The amplitude is:

$$A_7 = [A^{\omega}(111) \otimes A^{f_2}(220)]A^{\overline{p}p}(101) \tag{5}$$

where $\otimes$ denotes a tensor product. Contributions from higher angular momenta ($L \geq 2$) are assumed to be negligible due to phase space limitation.

The damping factors $F_L(q)$ are given by [19]

$$F_0(q) = 1, \quad F_1(q) = \sqrt{\frac{2z}{z+1}}, \quad F_2(q) = \sqrt{\frac{13z^2}{(z-3)^2+9z}} \tag{6}$$

where $z = (\frac{q[MeV]}{197.3})^2$. The Breit-Wigner factors are given by

$$BW_L(m) = \frac{m_0\Gamma_0}{m_0^2 - m^2 - im_0\Gamma(m)} \tag{7}$$

where

$$\Gamma(m) = \Gamma_0 \frac{m_0}{m}\frac{q}{q_0}\frac{F_L^2(q)}{F_L^2(q_0)} \tag{8}$$

with m_0 and Γ_0 the nominal mass and width of the resonance and q_0 the corresponding decay momentum. For the initial $\overline{p}p$ system BW=1. The mass and width of f_2 are fixed at 1270 and 185 MeV. The mass and width of b_1 are fixed at 1235 and 155 MeV. For the $\pi\pi$ S-wave we adopt the parametrization K_1 from Au et al. [20] in terms of the S-wave phase shift δ and the inelasticity η in elastic $\pi\pi$ scattering, and replace the Breit-Wigner amplitude by

$$BW_0(m) = \frac{m}{q}(\frac{\eta\exp(2i\delta) - 1}{2i}). \tag{9}$$

The transition probability w is then given by the coherent sum of all amplitudes

$$w = w_{PS} \times Tr|\sum_{j=1}^{7} \alpha_j A_j|^2 \tag{10}$$

where w_{PS} is the phase space weight and $\alpha_j = a_j\exp(i\phi_j)$ are unknown constants. The weight w can be rewritten in terms of the real constants a_j and ϕ_j to be determined by the fitting procedure:

$$w = \sum_i a_i^2 P_{ii} + 2\sum_{i<j} a_i a_j \mathrm{Re}[P_{ij}]\cos(\phi_i - \phi_j) + 2\sum_{i<j} a_i a_j \mathrm{Im}[P_{ij}]\sin(\phi_i - \phi_j) \tag{11}$$

where

$$P_{ij} = w_{PS} \times Tr(A_i A_j^{\dagger}). \tag{12}$$

One phase ϕ_j being arbitrary, we choose $\phi_1 = 0$. This leads to 7 parameters a_j and 6 phases ϕ_j.

We consider only the Dalitz plot (fig. 2a) and ignore for the fit the additional information on the angular distribution of the γ from ω decay. The fit predictions are then compared to

the γ angular data as a consistency check. An analysis of a ten times larger $\omega\pi^0\pi^0$ sample, including the γ angular distribution, is in progress and will be published later.

The Dalitz plot is folded around the main diagonal and divided into 265 cells, 0.065×0.065 GeV^4 wide. A constant background (7 events) is subtracted from each cell to take into account the 10% uniform backgound distribution of 7γ events. Cells with less than 5 events are not used in the fit. They are mainly distributed along the periphery of the Dalitz plot and are correctly described by the fit. This leaves 234 cells for a total N_T=15'032 $\omega\pi^0\pi^0$ events.

Monte Carlo Dalitz plots weighted by P_{ij} are generated for each pair i,j $(i \leq j)$. The P_{ij} (eq. 12) and correspondingly the weight w (eq. 10), are normalized to the total number of events N_T:

$$P_{ij} \rightarrow P_{ij}/\sqrt{f_i f_j} \tag{13}$$

with

$$f_i = \sum P_{ii}/N_T \tag{14}$$

where the sum extends over all (8×10^4) Monte Carlo events. We then build the χ^2

$$\chi^2 = \sum \frac{(n-w)^2}{n+\sigma_w^2} \tag{15}$$

where the sum extends over the contents n of 234 cells and σ_w are the statistical errors on the Monte Carlo weights.

The first fit uses the $\pi\pi$ S-wave amplitude from Ref. [20] (solution K_1) and leads to a χ^2/dof of 1.66 for 221 dof. The main features of the Dalitz plot are explained as follows: the depletion at the center of the Dalitz plot is due to destructive interference between the b_1 bands for each of the $L = 2$ amplitudes A_3 and A_4, and to destructive interference between the b_1 bands and the $\pi\pi$ S-wave which is strong near 750 MeV. As a result, the $b_1(1235)$ peak moves down in mass. The interference with the $\pi\pi$ S-wave is responsible for the reduction of the b_1 intensities at low $\pi\pi$ masses. The enhancement in the region where the b_1 bands intersect is due to interference with $f_2(1270)$.

The D/S ratio of $\ell = 2$ to $\ell = 0$ amplitudes for b_1 decay can be obtained from the ratio

$$D/S = \frac{1}{\sqrt{5}} a(\ell = 2)/a(\ell = 0). \tag{16}$$

We obtain $D/S = 0.68 \pm 0.14$ for $L = 0$, and $D/S = 0.40 \pm 0.05$ for $L = 2$. The D/S ratio has not been measured before in $\bar{p}p$ annihilation. The world average from b_1 production in πp and γp interactions is 0.26 ± 0.04 [15]. Since the D/S ratios are in fair agreement for $L = 0$ and $L = 2$, we repeat the fit by constraining them to be equal and obtain D/S=0.45$\pm$ 0.04 (fit A1). This leaves 12 free parameters and the χ^2 does not change significantly (χ^2/dof = 1.66 for 222 dof). The amplitudes and phases are given in table 1.

To compare the fit predictions with mass projections and since the fits have been performed on the background-free Dalitz plot, we have subtracted from the data in fig. 2b and c a 10% contribution of phase-space-distributed $\omega\pi^0\pi^0$ events. The grey areas in fig. 2b and c show the predictions from fit A1. The agreement with data is good except in the $\pi\pi$ mass spectrum around 1 GeV. All residuals are uniformly distributed across the Dalitz plot.

The dip in the 2π-mass distribution around 1 GeV is produced (i) by the $\pi\pi$ S-wave amplitude A_5 (destructive interference between the broad $\epsilon(750)$ and the narrow $f_0(975)$ [20]) and (ii) by the amplitude A_7 which increases with $\pi\pi$ mass (tail of $f_2(1270)$). The data however

show a more pronounced dip displaced by 40 MeV below prediction. The precise location of the minimum may depend on the $\pi\pi$ S-wave parametrization and on the $f_2(1270)$ width which is not accurately known. Accordingly, we have tried to match the observed minimum by using the alternative solution K_3 of Ref. [20] and have also varied the $f_2(1270)$ width. None of these attempts were successful in matching the dip position.

We have also tried an additional Breit-Wigner scalar contribution to the $\pi^0\pi^0$ mass spectrum around 1050 MeV. The mass was varied between 1000 and 1100 MeV and the width between 50 and 200 MeV. The χ^2/dof decreased to 1.47 although the fit was not very sensitive to the precise mass and width. The dip moved to lower masses and became broader, in accord with data, but the additional scalar contribution remained small (10% of the $f_2(1270)\omega$ intensity). The procedure is however not rigorous as it may violate unitarity and we therefore regard this attempt as inconclusive.

A similar shift is also observed in our data for $\bar{p}p \to 3\pi^0$ and $\eta\pi^0\pi^0$ [21]. The precise dip position depends on the couplings to $\epsilon(750)$ and $f_0(975)$ which may be different in $\bar{p}p$ and in $\pi\pi$ scattering. A more detailed K-matrix description including $K\overline{K}$ production introduces six additional free parameters and will be published later with the larger statistical sample. On the other hand, the results presented in this letter are not sensitive to the dip position. The solid line in fig. 2c shows the result of fit A2 in which the $f_0(975)$ mass is reduced by 40 MeV by rescaling the $\pi\pi$ amplitude. Fits A1 and A2 (table 1) give rather similar results.

We then introduce an amplitude B for the production and decay of a vector meson $\rho' \to \omega\pi$. Conservation of parity requires $L = \ell = 1$. In a first attempt we introduce a ρ' with mass 1270 MeV and width 166 MeV. This state was reported recently by LASS in $\pi^+\pi^-$ from an analysis of the reaction $K^-p \to \pi^+\pi^-\Lambda$ [22]. The amplitudes remain reasonably stable while the intensity b^2 for ρ' production is nearly consistent with zero (Fit B1 of table 1). A vector meson at 1256 MeV with a width of 130 MeV was also required in $\bar{p}p \to \omega\pi^+\pi^-$ [3]. The $L = 2$ amplitude $A4$, which we find rather strong (see table 1), and the amplitude $A6$ were however neglected in this analysis.

The contribution of a $\rho(1450)$ with a width of 310 MeV [5] is also nearly consistent with zero (fit B2). Vector states like C(1480) decaying to $\phi\pi$ but not to $\omega\pi$ [23] cannot be $q\bar{q}$. They could be produced in the annihilation channel $\phi\pi^0\pi^0$ but should be suppressed in $\omega\pi^0\pi^0$. Introducing the C(1480) with a width of 130 MeV [23] leads to amplitudes very similar to fit B2 and to an intensity consistent with zero.

Next, we introduce a contribution from the tail of $\rho(770)$ (fit B3). The χ^2 decreases significantly while the significance of b^2 is only 3σ. Figure 3 shows the ϕ- distribution of the γ in the mass range $m^2_{\omega\pi^0} < 1.12$ GeV^2 which is sensitive to a $\rho(770)$ contribution. The angle ϕ refers to the azimuthal angle of the γ with respect to the normal to the plane spanned by the three momentum vectors of the $\omega\pi^0\pi^0$ event. The prediction from fit A1 (grey area) is in reasonable agreement with the data, although possible structure cannot be resolved due to statistical limitations. Fit B3 however predicts oscillations in ϕ for which no evidence is seen in the data (solid line in fig. 3). We shall therefore only quote an upper limit for $\rho(770) \to \omega\pi$.

The data presented here are taken from a sample of 0-prong annihilations. The absolute number of stopped antiprotons is calculated by reconstructing annihilation events from the channel $\bar{p}p \to \pi^0\pi^0$ in the same data set (16'996 $\pm$ 466 events) and by using the absolute branching ratio for $\pi^0\pi^0$, (6.93 $\pm$ 0.43) $\times 10^{-4}$, which was determined earlier by this collaboration [24]. With a reconstruction efficiency of 0.47 $\pm$ 0.02 for $\pi^0\pi^0$ events one finds a total of N = (52.7 $\pm$ 3.6) $\times 10^6$ annihilations in liquid hydrogen. The ratio of 0-prong annihilations (2.05 $\times 10^6$) to the total number of annihilations N is (3.9 $\pm$ 0.3) %, in excellent agreement with the

known 0-prong branching ratio $(4.1\ ^{+0.2}_{-0.6})\%$ [25]. The branching ratio for $\omega\pi^0\pi^0$ is given by

$$B(\overline{p}p \to \omega\pi^0\pi^0) = \frac{N_0}{\epsilon B(\omega \to \pi^0\gamma)N} \tag{17}$$

where N_0 is the number of $\omega\pi^0\pi^0$ events (15'153 $\pm$ 147), ϵ the reconstruction efficiency, (16.9 $\pm$ 0.8) %, and B the branching ratio for ω decay into $\pi^0\gamma$, (8.5 $\pm$ 0.5) %. This leads to the branching ratio

$$B(\overline{p}p \to \omega\pi^0\pi^0) = (2.00 \pm 0.21)\% \tag{18}$$

which is determined for the first time.

The branching ratios for annihilation into $b_1(1235)\pi$, $\omega(\pi\pi)_S$ and $f_2(1270)\omega$ are in principle not uniquely defined due to interferences between the three channels. We define the branching ratio, relative to $\omega\pi^0\pi^0$, as the sum of the contributing intensities a_i^2 normalized to the total incoherent intensity $\sum_{i=1}^{7} a_i^2$, thereby ignoring interference effects. We find, using the amplitudes from fit A1 (table 1):

$$B(\overline{p}p \to \omega[\pi^0\pi^0]_S) = (0.51 \pm 0.07)\% \tag{19}$$

$$B(\overline{p}p \to b_1\pi^0, b_1 \to \omega\pi^0) = (0.92 \pm 0.11)\% \tag{20}$$

$$B(\overline{p}p \to f_2\omega, f_2 \to \pi^0\pi^0) = (0.57 \pm 0.07)\% \tag{21}$$

The branching ratios include all ω decay modes. The branching ratio for $f_2\omega$, corrected for all f_2 decay modes, is (2.01 $\pm$ 0.25) %.

The branching ratio for the channel $\omega\pi^+\pi^-$ was determined earlier by a bubble chamber experiment [2] as (6.6 $\pm$ 0.6) %, with contributions from $\omega\rho^0$ (2.26 $\pm$ 0.23) %, $b_1^{\pm}\pi^{\mp}$ (0.79 $\pm$ 0.11) %, $\omega(\pi^+\pi^-)_S$ (3.29 $\pm$ 0.33) % and $f_2\omega$ (3.26 $\pm$ 0.33) %. Subtracting from the $\omega\pi^+\pi^-$ branching ratio the $\pi^+\pi^-$ P-wave contribution ($\omega\rho^0$ rate), one predicts for $\omega\pi^0\pi^0$ a branching ratio of (2.2 $\pm$ 0.2) %, in excellent agreement with our result. The figure for $b_1^{\pm}\pi^{\mp}$ refers to the total rate for both charged b_1. Our value for $b_1^0\pi^0$ is larger while our branching ratios for $f_2\omega$ and $\omega(\pi^0\pi^0)_S$ are smaller. We emphasize, however, that the rates are defined neglecting interferences which are different for the charged and neutral channels.

Upper limits for the production and decay rates of vector mesons can be given using the amplitudes from table 1 and the branching ratio for $\omega\pi^0\pi^0$. We find (95% confidence level upper limit):

$$B(\overline{p}p \to \rho(1270)\pi^0, \rho(1270) \to \omega\pi^0) < 7 \times 10^{-4}, \tag{22}$$

$$B(\overline{p}p \to \rho(1450)\pi^0, \rho(1450) \to \omega\pi^0) < 3 \times 10^{-4}, \tag{23}$$

$$B(\overline{p}p \to \rho(770)\pi^0, \rho(770) \to \omega\pi^0) < 9 \times 10^{-4}, \tag{24}$$

$$B(\overline{p}p \to C(1480)\pi^0, C(1480) \to \omega\pi^0) < 6 \times 10^{-5}. \tag{25}$$

Summarizing, we have performed a Dalitz plot analysis of the annihilation channel $\overline{p}p \to \omega\pi^0\pi^0$. This channel is dominated by the production of $b_1^0(1235)$ and no additional state decaying to $\omega\pi$ is observed. The contribution from vector mesons is negligible. The $2\pi^0$-mass spectrum is dominated by the $\pi\pi$ S-wave and by the tail of $f_2(1270)$, largely responsible for the peak observed around 1050 MeV.

We would like to thank the technical staff of the LEAR machine group and of all the participating institutions for their invaluable contributions to the success of the experiment. We acknowledge financial support from the German Bundesministerium für Forschung und

Technologie, the Schweizerischer Nationalfonds, the British Science and Engineering Research Council and the U.S. Department of Energy (contract No. DE-FG03-87ER40323 and DE-AC03-76SF00098). J.K. acknowledges support from the Alexander von Humboldt Foundation and K.K. from the Heisenberg Foundation.

References

[1] G. Reifenröther and E. Klempt, Phys. Lett. B245 (1990) 129
[2] R. Bizzarri et al., Nucl. Phys. B14 (1969) 169
[3] P. Frenkiel et al., Nucl. Phys. B47 (1972) 61
[4] P. Weidenauer et al., Z. Phys. C (in print)
[5] A. Donnachie et al., Z. Phys. C51 (1991) 689
[6] C.B. Dover and J.M. Richard, Ann. Phys. NY 121 (1979) 47, 70
[7] B. May et al., Phys. Lett. B225 (1989) 450, Z. Phys. C46 (1990) 191, 203
[8] E. Aker et al., Phys. Lett. B260 (1991) 249
[9] L. Gray et al., Phys. Rev. D27 (1983) 307
[10] C.B. Dover et al., Phys. Rev. C43 (1991) 379
[11] J. Diaz et al., Nucl. Phys. B16 (1970) 239
[12] I. Daftari et al., Phys. Rev. Lett. 58 (1987) 859
[13] E. Aker et al., Nucl. Instr. Methods A321 (1992) 69
[14] R. Brun et al., Internal Report CERN DD/EE/84- 1, CERN 1987
[15] Review of Particle Properties, Phys. Rev. D45 (1992) Part II
[16] C. Amsler et al., submitted to Z. Phys. C, preprint CERN-PPE/93-11
[17] M. Jacob and G.C. Wick, Ann. Phys. 7 (1959) 401
[18] C. Amsler and J.C. Bizot, Comp. Phys. Comm. 30 (1983) 21
[19] F.v. Hippel and C. Quigg, Phys. Rev. D5 (1972) 624
[20] K.L. Au et al., Phys. Rev. D35 (1987) 1633
[21] C. Amsler et al., in preparation
[22] D. Aston et al., Nucl. Phys. B (Proc. Suppl.) 21 (1991) 105
[23] S.I. Bityukov et al., Phys. Lett. B188 (1987) 383
[24] C. Amsler et al., Phys. Lett. B297 (1992) 214
[25] C. Ghesquière, Symp. on Antinucleon Nucleon Interactions, Liblice, CERN Yellow Report 74-18 (1974) p. 436

Table 1: Results of various Dalitz plot fits assuming the $b_1(1235)$ D/S ratios equal for $L = 0$ and 2. Fit A1 refers to the minimum assumption with no additional contribution and fit A2 to the rescaled $\pi\pi$ amplitude. Fit B1 refers to inclusion of $\rho(1270)$, B2 to $\rho(1450)$ and B3 to $\rho(770)$ decaying to $\omega\pi$.

		A1	A2	B1	B2	B3
χ^2/dof		1.66	1.52	1.60	1.63	1.46
dof		222	222	220	220	220
$b_1\pi^0$	D/S	.45 (.04)	.44 (.04)	.48 (.04)	.45 (.03)	.46 (.04)
	$a_1(L=0)$	.26 (.02)	.30 (.02)	.20 (.03)	.25 (.03)	.19 (.02)
	$a_3(L=2)$	.48 (.04)	.45 (.04)	.46 (.04)	.46 (.03)	.48 (.03)
	ϕ_2	3.45 (.39)	3.98 (.38)	3.26 (.51)	3.39 (.46)	2.71 (.57)
	ϕ_3	.17 (.26)	.71 (.25)	-.06 (.39)	.34 (.37)	.16 (.31)
	ϕ_4	.58 (.16)	1.33 (.16)	.28 (.29)	.61 (.25)	.28 (.26)
$\omega(\pi^0\pi^0)_S$	$a_5(L=0)$	.57 (.02)	.53 (.02)	.56 (.02)	.55 (.02)	.56 (.03)
	$a_6(L=2)$	.10 (.05)	.13 (.05)	.09 (.05)	.15 (.05)	.19 (.07)
	ϕ_5	1.12 (0.10)	1.38 (.08)	.79 (.23)	1.01 (.16)	1.13 (.18)
	ϕ_6	5.57 (.41)	6.03 (.38)	5.17 (.50)	5.39 (.40)	2.76 (.32)
$f_2\omega$	a_7	.61 (.02)	.63 (.02)	.59 (.03)	.60 (.02)	.62 (.02)
	ϕ_7	2.37 (.25)	2.96 (.26)	2.38 (.34)	2.81 (.31)	2.31 (.32)
ρ'	b			.14 (.05)	.09 (.03)	.19 (.03)
	ϕ_b			-.88 (.42)	-.05 (.37)	-.68 (.27)

Figure captions

Figure 1: (a) Energy distribution of the single γ for events kinematically fitted to the hypothesis $\overline{p}p \to 3\pi^0\gamma$; (b) $\pi^0\gamma$-invariant mass distribution (3 entries/event). The inset shows the fit to the ω signal.

Figure 2: (a) Dalitz plot for $\overline{p}p \to \omega\pi^0\pi^0$ (2 entries per event). The population increases from white to black in steps of 30 entries/cell, each cell being 0.065×0.065 GeV^4 wide (statistical fluctuations in the contour lines have been smoothed out); (b) $\pi^0\omega$ invariant mass projection (2 entries per event); (c) $\pi^0\pi^0$ invariant mass projection. In (b) and (c) the dots represent the data, the grey areas the result of the Dalitz plot fit A1 and the solid line the result of fit A2 described in the text.

Figure 3: ϕ-angular distribution of the γ from ω decay for events with $m^2_{\omega\pi^0} < 1.12$ GeV^2. The grey area shows the predictions from fit A1 and the solid line the prediction from fit B3 which includes a contribution from $\rho(770)$ decay to $\omega\pi^0$.

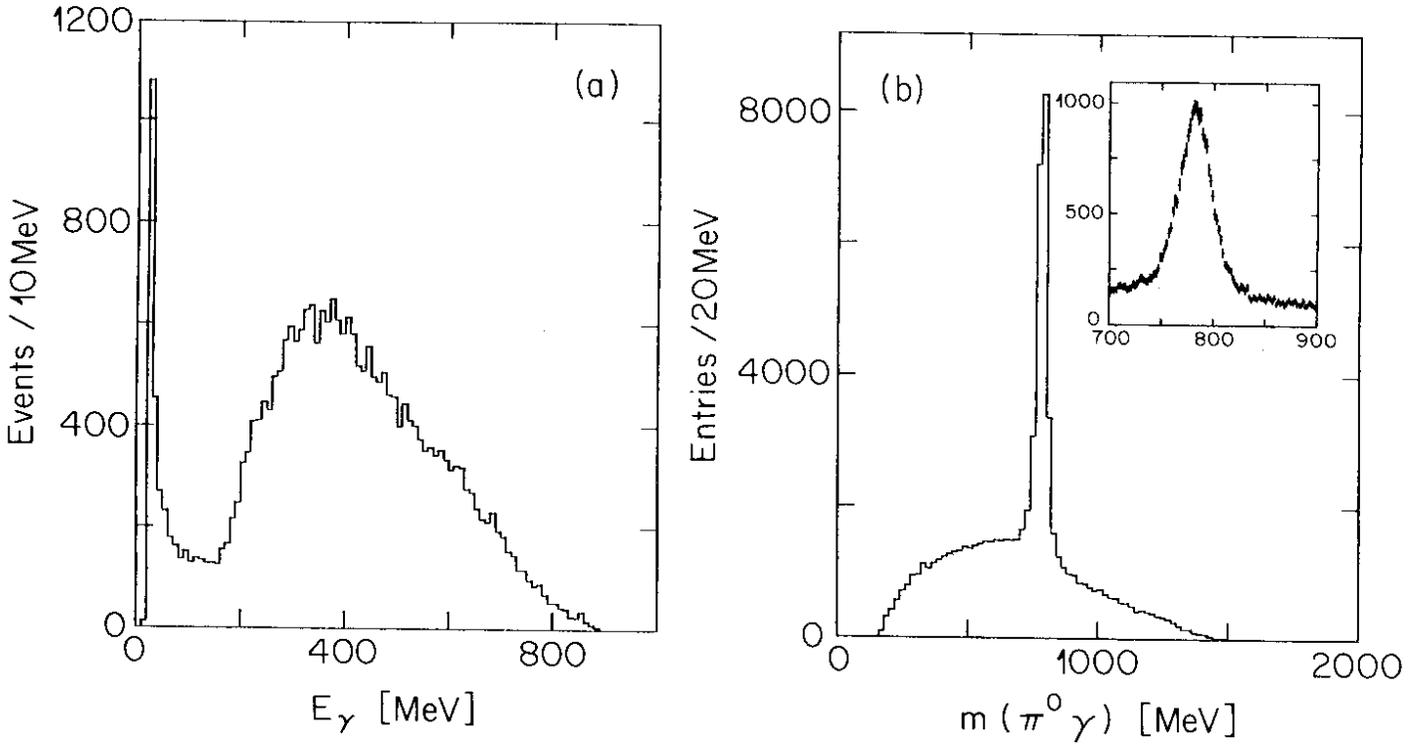
(a)
Events / 10MeV
1200
800
400
0
0
400
800
E_γ [MeV]
(b)
Entries / 20MeV
8000
4000
0
0
1000
2000
$m(\pi^0\gamma)$ [MeV]
1000
500
0
700
800
900

Fig. 1

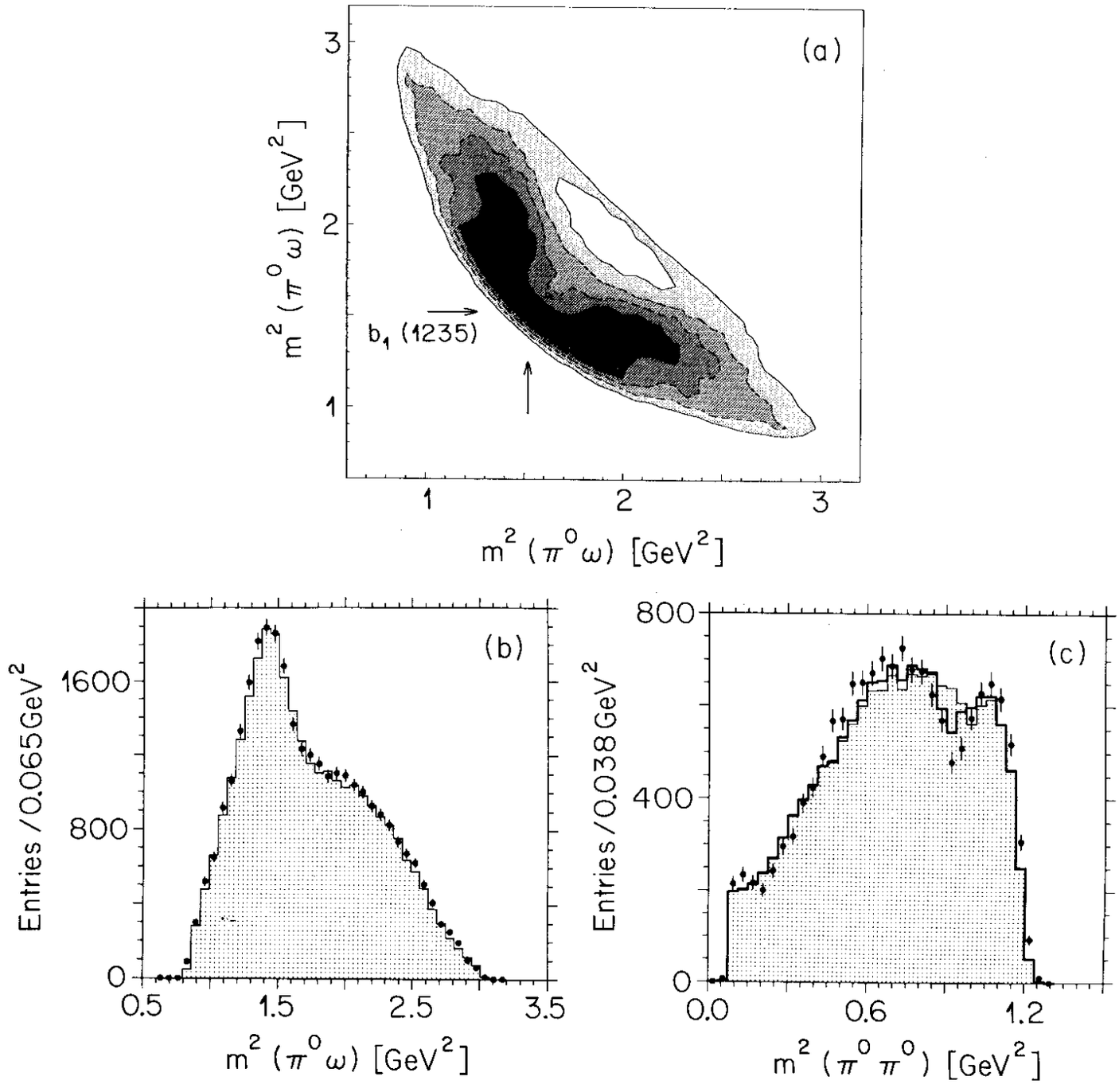
(a)
$m^2(\pi^0\omega)$ [GeV^2]
b_1 (1235)
$m^2(\pi^0\omega)$ [GeV^2]
(b)
Entries /0.065GeV^2
$m^2(\pi^0\omega)$ [GeV^2]
(c)
Entries /0.038GeV^2
$m^2(\pi^0\pi^0)$ [GeV^2]

Fig. 2

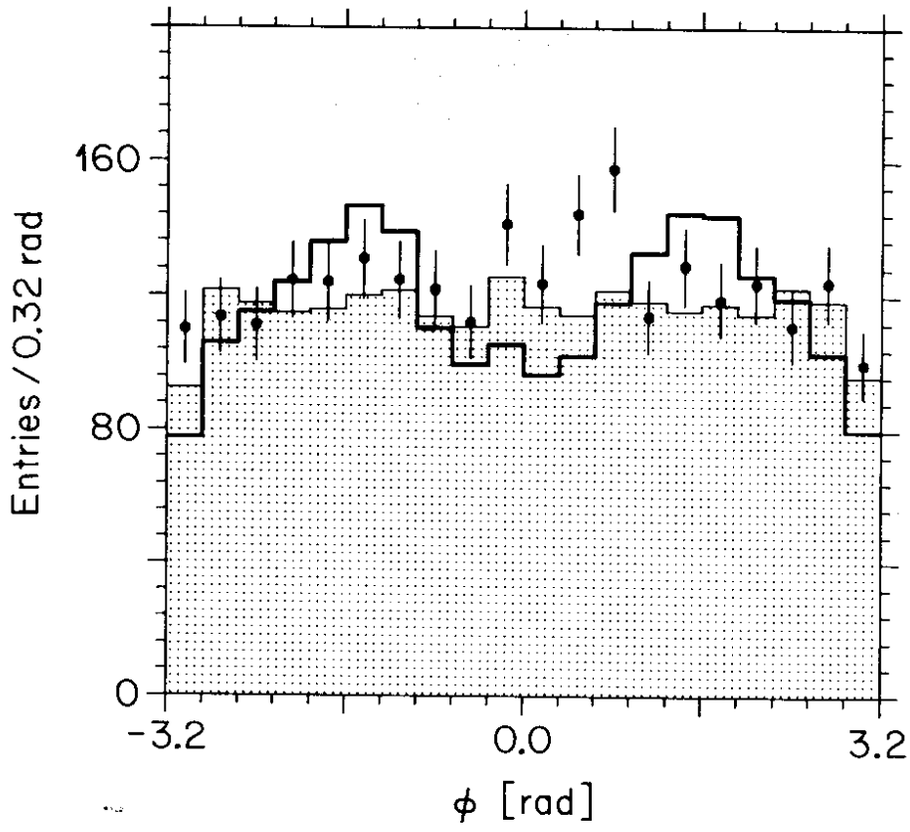

Fig. 3